Identification of Carotid Plaques Composition Through a Compact CSRR-Based Microwave Sensor

Rania Shahbaz, Frédérique Deshours, Georges Alquié, Hamid Kokabi, Fabien Koskas, Isabelle Brocheriou, Gilles Le Naour, Chaouki Hannachi, Jean-Michel Davaine

Version of Record: https://www.sciencedirect.com/science/article/pii/S1959031822000823
Manuscript_03ec995dba4c468c1264e1ab60ce1083

Identification of Carotid Plaques Composition through a Compact CSRR-Based Microwave Sensor

R. Shahbaz[a*], F. Deshours[a], G. Alquie[a], H. Kokabi[a], F. Koskas[b], I. Brocheriou[c],

G. Le Naour[c], C. Hannachi[a], J-M. Davaine[b]

[a] *Sorbonne Université, CNRS, Laboratoire Génie Électrique et Électronique de Paris, Paris*
[b] *Sorbonne Université, Service de chirurgie vasculaire, Pitié Salpêtrière, Paris*
[c] *Sorbonne Université, Service d'Anatomie et cytologie pathologiques, Pitié Salpêtrière, Paris*

Abstract

Objectives: This study aims to identify the dielectric constant of the carotid atherosclerotic plaques and categorise them using a CSRR based microwave sensor.

Material and methods: A Complementary Split Ring Resonator (CSRR) at 2.3 GHz measured 33 samples of carotid plaques obtained after endarterectomy. HFSS software simulations were employed to substantiate the measurements. Histological analyses were performed simultaneously to classify the plaques.

Results: The constant dielectric of dangerous carotid plaques identified by histology was much higher than that of low-risk calcified carotid plaques. Microwave data were pertinent to the simulations.

Conclusion: The current study, performed on ex-vivo carotid plaques, illustrates the sensor's ability to differentiate plaques with diverse components. Calcified low-risk plaques displayed distinct values from dangerous soft plaques. Further statistical correlation of the 33 samples is required. After validation, an in-vivo prototype will be designed and tested.

Keywords: Biosensor, Carotid Plaque, CSRR, Microwave, Resonator.

1. Introduction

Advancements in the medical treatment of atheromatous diseases by OMT (Optimal Medical Therapy) in the last few years have made the surgical indications for Carotid Endarterectomy (CEA) questionable and ambiguous [1, 2]. Atheromatous carotid stenosis causes 20% to 30% of ischemic strokes and is detected in a large number of asymptomatic patients over the age of 50 [3]. Historically, CEA indications were based on studies using arteriography to evaluate the lesion. However, arteriography does not permit the comprehensive exploration of the plaque structure; it provides only the degree of stenosis associated with the risk of a cardiovascular event [4].

∗Corresponding author.
Email address: rania.shahbaz@sorbonne-universite.fr (Rania Shahbaz)

Nevertheless, it is widely recognised today that other parameters, particularly the composition of the plaque and its vulnerability, play a critical role in the clinical behaviour of carotid atherosclerotic plaques.

The current indications are based on randomised trials held in the 1990s [5, 6], which established the benefit of the intervention on "symptomatic" (minor ischemic attack) and "asymptomatic" stenosis with a degree of stenosis (easily measurable by echo-Doppler, angio-CT or angio-MRI) greater than 70% [7]. For beyond this figure, the risk of stroke is greater than the surgical risk, and the inaugural ischemic attack is usually severe in around 50% of the cases. These factors justify preventive surgery for "asymptomatic" patients, albeit the benefit of surgery, i.e. CEA became debatable with recent advances in medical treatment [8].

Moreover, the degree of stenosis alone does not scrutinise carotid atheromatous plaque's physiological, anatomical, and hemodynamic complexity [7, 9]. It is acknowledged that the plaque composition in lipid, calcium, and/or fibrous tissue strongly influences its clinical behaviour. In particular, the calcium component of an atherosclerotic plaque, both at the early and late stages of its formation, strongly influences the wall's stiffness, the stability of the plaque, and its risk of rupture [10, 11]. Furthermore, the hemodynamic significance of carotid stenosis routinely based on diameters (NASCET) [5] is conceptually out of date as it is incongruent when compared to the overall visualisation of the arterial circulation of the neck and the brain (the Willis system).

The modalities currently used to preoperatively evaluate carotid plaque lesions are multi-detector CT scanner (MDCT), Doppler ultrasound and MRI. Currently, none of these modalities can precisely define the carotid plaque composition. They mainly show plaque morphology and luminal stenosis. Presently, the gold standard and the only technique to characterise the plaque composition, therefore vulnerability, is histology. Current medical research recognises thin fibrous cap, sizeable necrotic core, and intra-plaque haemorrhage (IPH) as the optimal markers of vulnerable plaques [12–15].

As a result, innovative and non-invasive techniques to estimate the aggressiveness and scalability of carotid plaques and, hence, establish the indications for CEA are highly needed.

Various techniques for detecting and identifying elements have been developed in recent years. Approaches utilising microwave sensors have garnered considerable interest due to their ability to penetrate various materials and sense from a distance by dielectric contrast [16]. Microwave measurements of permittivity are critical and widespread in many fields, including medicine and health care [17].

Free-space, near-field, transmission line, and resonance-based techniques are all types of RF and microwave approaches. Resonance-based approaches are generally selected because of their high accuracy, great sensitivity, and low cost [17]. Resonant sensors' non-invasive and non-destructive character made them a better choice than non-resonant ones due to their superior precision within a narrow frequency band. Moreover, planar structures based on metamaterials have been developed to investigate specific liquids' contactless dielectric properties or be used as gas sensors [18-20]. Compared to the conventional structure of planar resonators, their interest

enabling relatively localised measurements.

Typically, two forms of compact quasi-static resonators have been widely used for characterising materials, SRRs (Split Ring Resonator) and their complementary CSRR. Due to the electromagnetic excitation with the electric field parallel to the axis of symmetry, CSRRs are more sensitive to the dielectric permittivity of the surrounding medium in the near field than in the far-field measurements.

When covering the resonator with a dielectric material (here, the carotid plaque), its permittivity $\sum_r$ induces a frequency shift towards lower frequencies, increasing with the permittivity value. Therefore, this device can hypothetically distinguish highly calcified plaques from risky soft plaques. This paper evaluates the composition of the atheromatous biological tissue through ex-vivo measurements of the dielectric permittivity with our sensor and compares the results of histological analysis on the same samples. This study investigates the potential of this sensor to allow in-vivo preoperative exploration of atherosclerotic lesions in patients.

2. Medical methods

Samples from thirty-three patients (9 female / 24 male, mean age 71 ± 9 years) were included. Seven of them were symptomatic. All patients presented with a ≥ 70% carotid arterial stenosis determined by computed tomography angiography (CTA) & ultrasound imaging (NASCET criteria) and were scheduled for carotid endarterectomy (CEA) between January and December 2020.

Exclusion criteria consisted of prior carotid artery surgery on the same side, prior carotid artery endovascular procedures or prior cervical radiation. Patients were considered symptomatic if they had experienced a transient ischemic attack (TIA), amaurosis fugax (AF), central retinal artery occlusion (CRAO) or had a stroke ipsilateral to the carotid lesion that was being studied within three months prior to surgery. Silent infarcts and lacunar symptomatology, diagnosed by a neurologist based on a clinical and brain computer tomography (CT) scan and/or magnetic resonance imaging (MRI) located ipsilateral to the stenosis, were also considered symptomatic.

The institutional review board at "Hôpitaux Universitaires Pitié Salpêtrière - Charles Foix" approved the study, and patient consent was waived.

2.1. Carotid Endarterectomy (CEA)

Carotid plaques were extracted during the surgery by endarterectomy at the bifurcation from the lumen as a single specimen. The vascular surgeon then cut the plaque longitudinally, i.e. parallel to the lumen, into two identical samples (Figure 1. A). After removal, one sample was immersed in formalin and sent to the histology department. The second sample was immersed in physiological serum and reserved in suitable conditions. Since the microwave sensor was not situated in the hospital,

measurements.

All the surgical details were documented and entered in the excel sheet of the patient with the baseline data.

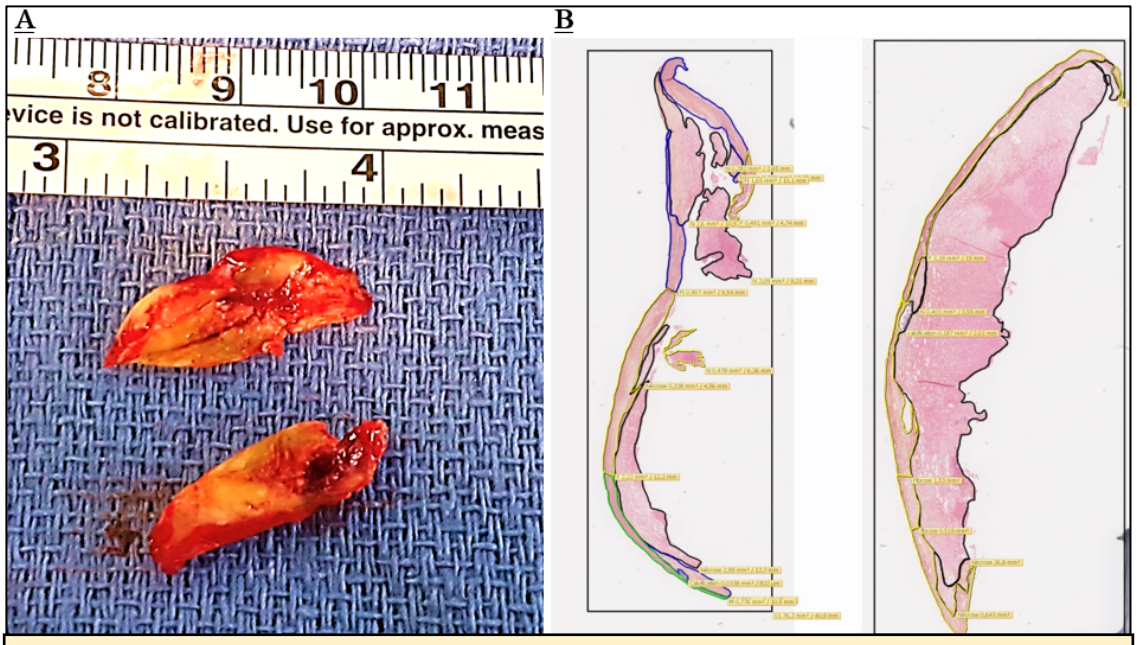

Figure 1. (A) Carotid plaque specimen of a symptomatic patient cut into two halves longitudinally. (B) Histological slide of the same sample outlined to indicate different areas of calcification, fibrous cap and lipid rich necrotic core.

2.2. Histology

Histological analysis was performed by an experienced histopathologist blind to the patients' clinical details. The samples were fixed in 10% buffered formalin, then decalcified (if necessary) with a decalcification solution (surgipath Decalcifier II-Leica), and immersed in paraffin. Histological sections with a thickness of 3 microns were prepared and stained with HES staining (Hematein, Eosin, Saffron). The total sectional area of each slide was scanned at 40X magnification with a resolution of 0.24 micron/pixel by a Nanozoomer Hamamatsu scanner. The digital slides were then viewed on high definition screens (BARCO Coronis Fusion) to locate the different types of tissues precisely. All regions were manually outlined with Viewer (NDP.view2) in order to obtain an accurate mapping and area of each component of the atherosclerotic plaque sample (Figure 1. B). This semi-quantitative analysis was performed to determine the presence of calcification (CAL), lipid-rich necrotic core (LRNC), intraplaque haemorrhage (IPH), and fibrous cap (FC).

3.1. Microwave measurements methodology

Microwave dielectric characterisation of carotid plaques is performed using a resonant method which gives better accuracy in obtaining dielectric parameters of materials even if they have high losses. In order to characterise ex-vivo relatively small samples of biological tissues (about one cm^2 of surface and 2 mm of thickness), a planar sensor was designed to fulfil these conditions; the resonance frequency was chosen in the Industrial, Scientific and Medical (ISM) frequency band for the relatively good penetration of microwaves into the biological tissues [18, 19] and the possibility to design resonant sensors with small dimensions and high-quality factor.

The energy stored by the resonant sensor is radiated inside the tissue applied on its surface, and the electric field interacts with the dielectric medium. As a result, the frequency of the sensor is modified. These changes can be quantified and determine the tissue's dielectric properties (permittivity and losses) [19, 20].

3.2 Design and realisation of Complementary Split Ring Resonator (CSRR)

The metamaterial-based resonant microwave sensor involves a Complementary Split Ring Resonator (CSRR) with a circular shape and two split ring resonators. The CSRR acts as a stop-band when it is excited by a time-varying electric field with a component parallel to its axis [21]. The CSRR is then engraved in the ground plane of a microstrip transmission line structure, which is well suited to the field geometry. This microstrip structure is matched to 50 Ω enabling microwave reflection and transmission measurements with a Vector Network Analyser (VNA).

Figure 2 & 3 represents the structure's design with the SMA accesses for measurements. The microstrip structure was realised on a commercial FR4 substrate with $\varepsilon_r = 4.6$, $\tan\delta = 0.02$ and a thickness of 0.73 mm; the metallisation thickness is $t = 35$ µm. The dimensions of the CSRR, given in Figure 2, are optimised with the HFSS Electromagnetic software in order to obtain in unloaded conditions a

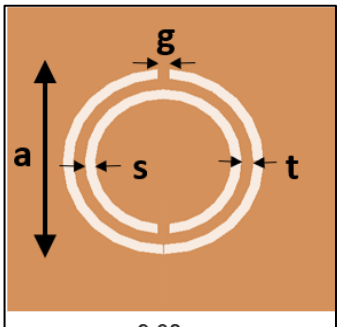

Figure 2. Geometric parameters of CSRR

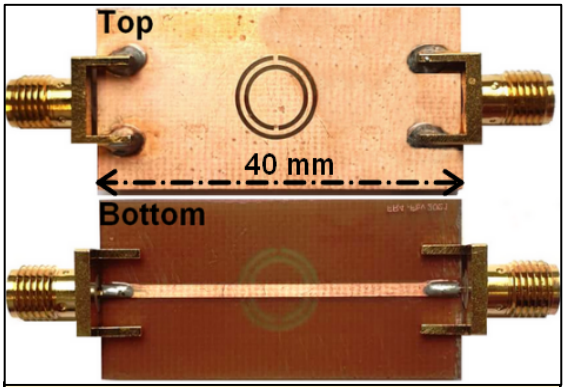

Figure 3. CSRR resonator on FR4 substrate

frequency range, the resonator's size is significantly small (~ 1 cm²) compared to conventional ones.

The designed CSRR sensor circuits were manufactured using an LPKF ProtoLaser S4 laser system equipped with an LPKF CircuitPro software. The system efficiently prototypes complex digital, analogue circuits and RF and microwave PCBs. It produces precise geometries on a range of substrates such as copper-clad FR4, aluminum-coated PET films, ceramics, Duroid, and PTFE. It is engraved in the ground plane of a microstrip structure [23]. Our team studied several resonator shapes thoroughly and chose the circular one for this study [22 - 25] due to its adequate performance and a better facility for testing biological tissues.

Furthermore, since biological tissues are relatively moist, a glass plate of $\varepsilon_{r\,v} = 7$, $\tan\delta = 0.02$ and 120 µm thickness was placed on the surface of the resonator in order to avoid short-circuiting between the slits. This insulating dielectric contributes to a lowering of 140 MHz of the resonant frequency. This frequency shift was verified using 3D full-wave electromagnetic field simulation software (HFSS & CST) and is considered in the measurements.

3.3 Electrical model of CSRR

An equivalent electrical model was developed for this resonator with and without biological samples. Since the geometric dimensions of the resonator are small compared to the wavelength, the value of the elements of the electrical equivalent schema was determined using quasi-static models for the constituent elements as well as by electrical simulations with ADS. The values of the elements of the studied resonator were obtained from S parameters measurements of the structure after de-embedding of the access lines. The equivalent RLC electric model can be extracted from it, making it possible to specify the resonant frequency (Figure 4). In the absence of the biological sample, the resonant frequency is given by equation (1):

$$f_0 = \frac{1}{2\pi\sqrt{L_R\left(C_R + C_C\right)}} \quad (1)$$

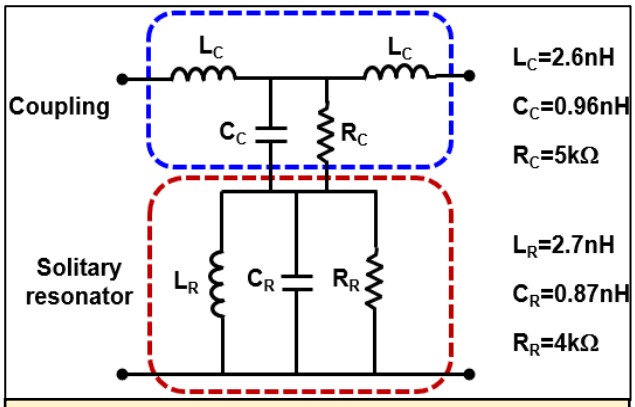

Figure 4. Equivalent electrical schema of the resonator

extracted from characteristic frequencies measured on the S-parameters and on the Z11 input impedance. The principle of extraction was also explained [22]. The results of the modelling by ADS and simulations by HFSS are compared with the experimental measurements in Figure 5.

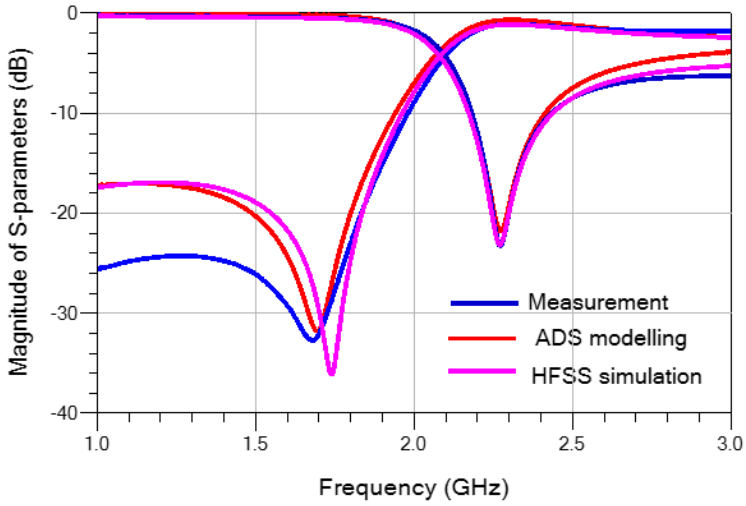

Figure 5. Graph comparing the modelling on ADS with the simulation on HFSS and the experimental measurements

3.4 Influence of the superstrate

When a microwave signal is supplied into a microstrip transmission line, it excites the CSRR by producing a voltage differential between the CSRR's capacitive rings and the ground plane [20, 21]. The presence of a dielectric sample (generally called superstrate) on the surface of the CSRR increases the capacitance C_R of the resonator as of equation (1). The resonant frequency is hence lowered, and the shift depends on the dielectric constant ε_{rs} of this superstrate.

Electromagnetic models with HFSS made it possible to verify this dependence and link the frequency shift with the dielectric constant of the superstrate for a

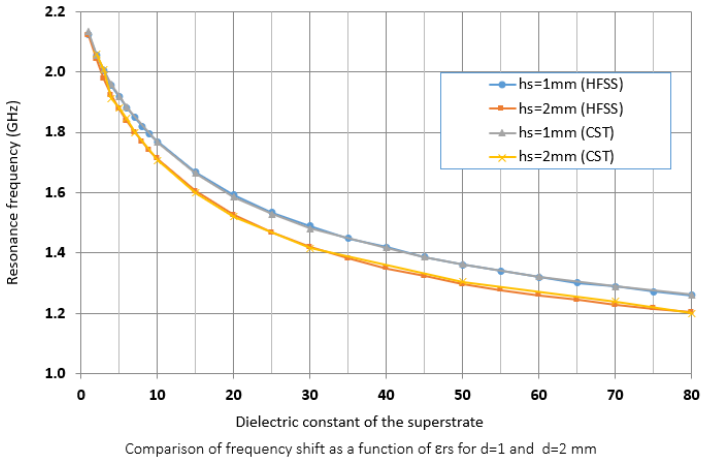

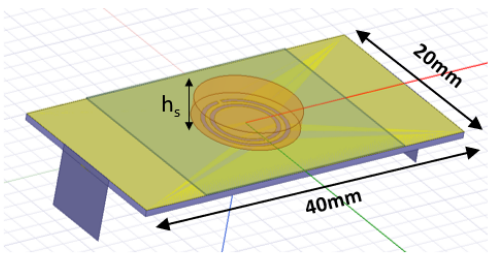

SUPERSTRATE:
h_s = 1mm ; 2mm
ε_{rs} = 1 to 10 (step 1)
ε_{rs} = 10 to 85 (step 5)
$\tan\delta_s$ = 0 ; 0.1 ; 0.2 and 0.3

Figure 6. CST and HFSS simulation results of mimicking samples of biological tissues with a thickness of 1 & 2 mm

simulations for samples having a dielectric constant ε_{rs} between 1 and 80; the resonance shift behaves roughly as $\varepsilon_{rs}^{1/2}$. Two sample thicknesses were simulated, i.e. 1 mm and 2 mm, representing approximately the range of thickness of our samples. The value of $|S_{21}|$ at resonance depends on sample losses as the Q-factor of the resonator since the losses of the superstrate lower the resistance RR and contribute to widening the resonance hollow.

3.5 Simulation results

The unloaded resonator (without sample) was simulated using HFSS, and the resonant frequency obtained was almost precisely the same as the one measured S_{21} ≈ 2.27 GHz. A Plexiglas structure designed in our lab to provide the rigid support necessary to perform reproducible measurements and a glass blade layer added to avoid short-circuiting between the rings were simulated with the resonator and resulted in a diminution of $\Delta f \approx 152$ MHz (Figure 7).

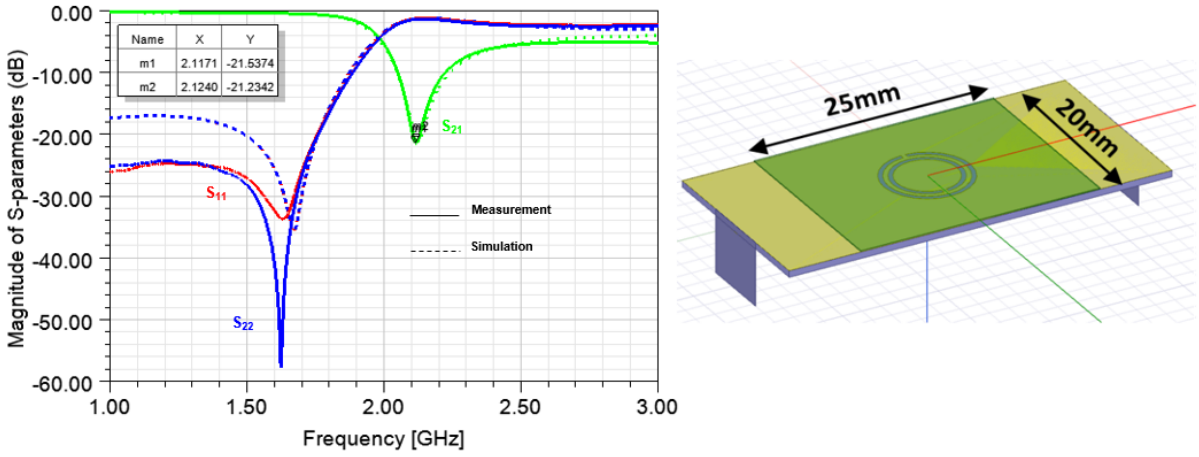

Figure 7. HFSS Simulation and measurement of the resonator + glass layer + plexiglass structure. S_{11}, S_{21}, and S_{22} were all taken into account, however only S_{21} was included in the analysis.
f_0 measured = m1 **f_0 simulated = m2**

3.6 Experimental setup

The sample extracted by endarterectomy was analysed within the same week of the surgical intervention. For the analysis, it was delicately dried from the physiological serum and cut in a uniform circle of 1 cm diameter at the narrowest part of the lesion (another circular sample is cut in the case of large plaques). The plaque thickness and weight were then measured. To avoid the humidity issue, the sample was left to dry for 3 minutes and then placed on the thin layer of glass on the resonator.

The Keysight PNA-L Network Analyser (300 kHz – 13.5 GHz) was calibrated for every set of measurements using a 3.5 mm calibration kit before it was connected

as a reference to ensure the baseline matching between measurements. The resonator would then be inserted into the plexiglass structure. At that point, the round-shaped atheroma plaque would be inserted (Figure 8) and covered with a piston made of Teflon to eliminate air and ensure good electrical contact with the glass cover of the resonator.

A light pressure of 300 g would always be applied on the piston that covered the sample to avoid the risk of deforming the plaque. The complete set of scattering parameters would then be recorded versus frequency for later analysis. The ambient and the samples temperature was maintained at 20 degrees Celsius for all measurements.

Figure 8. Sample holder setup with an atheromatous plaque

4. Results

Thirty-three samples were measured, and their parameters were extracted using HFSS. Samples had various frequency shifts and curve wideness. As expected, the dielectric constant ε_{rs} differed according to the composition of the plaque and in a less manner with the thickness of the sample, which was partially controlled by the pressure system. This was observed by considering the minimum frequency of the amplitude of the transmission coefficient $|S_{21}|$ parameter, which shifted to lower frequencies as ε_{rs} increased.

The results of the histological analysis were not entirely obtained during the production of this article; therefore, only three sample results are presented. The three samples represent three groups (risky plaque, stable plaque and mixed plaque).

minor frequency shifts (≈ frequency range 1.8 GHz), and its dielectric constant is closer to that of bone ($\varepsilon_r \approx 10$). In contrast, the much softer plaque (≈ frequency range 1.3 GHz) showed a higher frequency shift and a higher dielectric constant, confirming the presence of an intra-plaque haemorrhage and lipid-rich necrotic core.

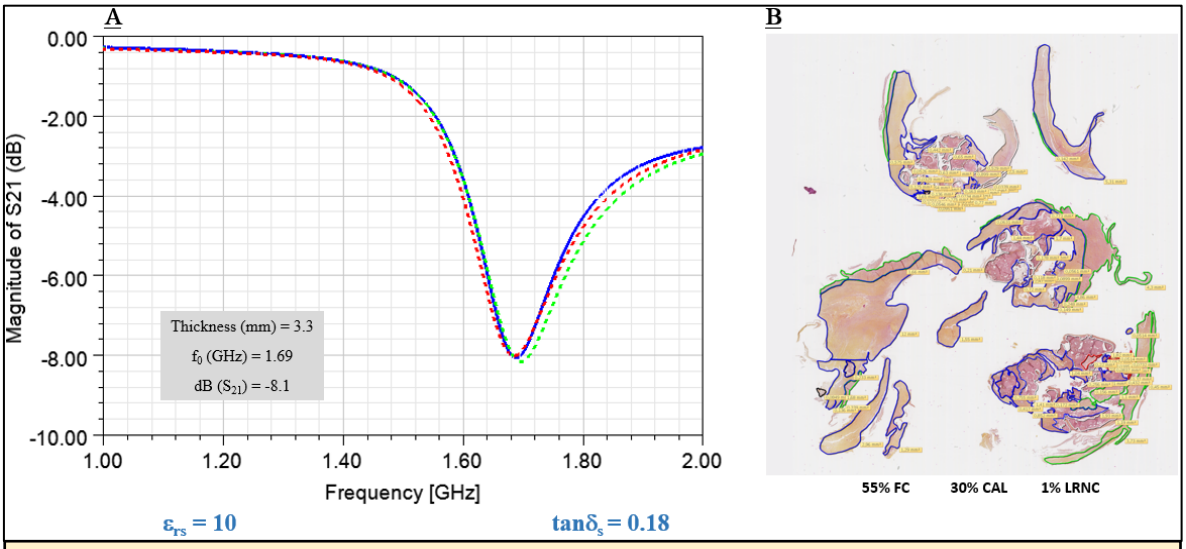

Figure 9. (A) S_{21} frequency response of a carotid plaque sample of an **asymptomatic patient**. (B) Histological slide analysis of the same patient.

Figure 9 displays the results of an asymptomatic patient who had an extremely rough plaque and presented a stable well-calcified plaque in histology. When measured with the microwave sensor, the sample caused a minor shift in frequency calculated into $\varepsilon_{rs} = 10$ whereas the symptomatic patient in Figure 10, who developed stroke symptoms a few weeks before the surgery, had a high ε_{rs} resulting from a much more significant frequency shift. Their histological analysis results correlated reasonably well with these findings. As in the asymptomatic patient, 30% CAL was calculated in addition to 55% FC; signs of stable plaque. In contrast, the symptomatic patient had a 48% LRNC; indicating a plaque at risk.

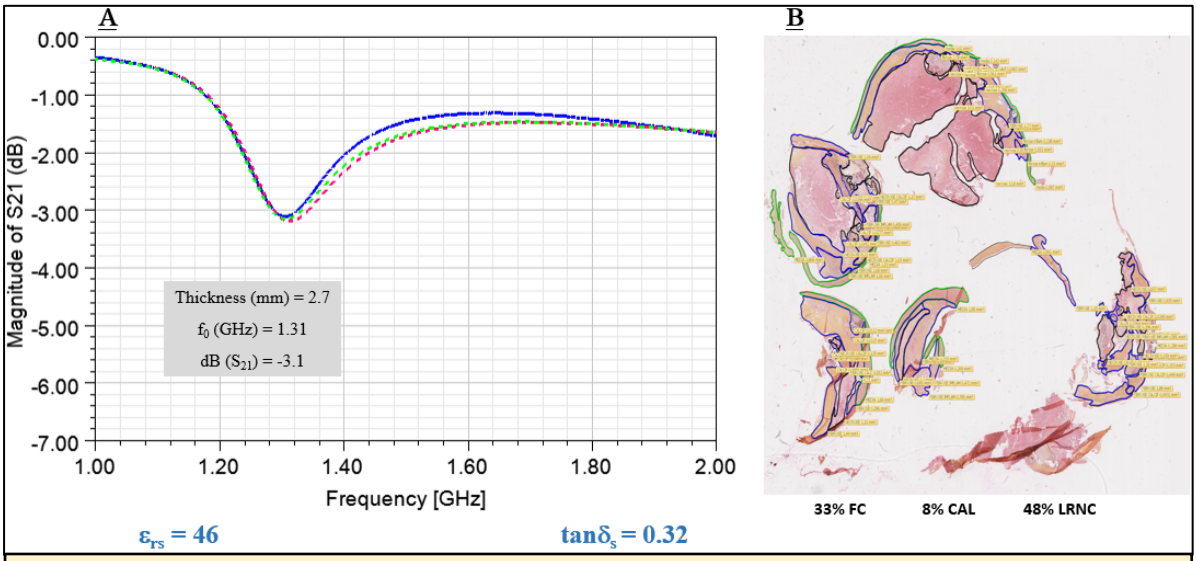

Figure 10. (A) S_{21} frequency response of a carotid plaque sample of a **symptomatic patient**. (B) Histological slide analysis of the same patient.

to the patient in Figure 11, who had an ε_{rs} = 27 and a 44% FC in histology and an adequate quantity of LRNC, which renders it an unstable plaque.

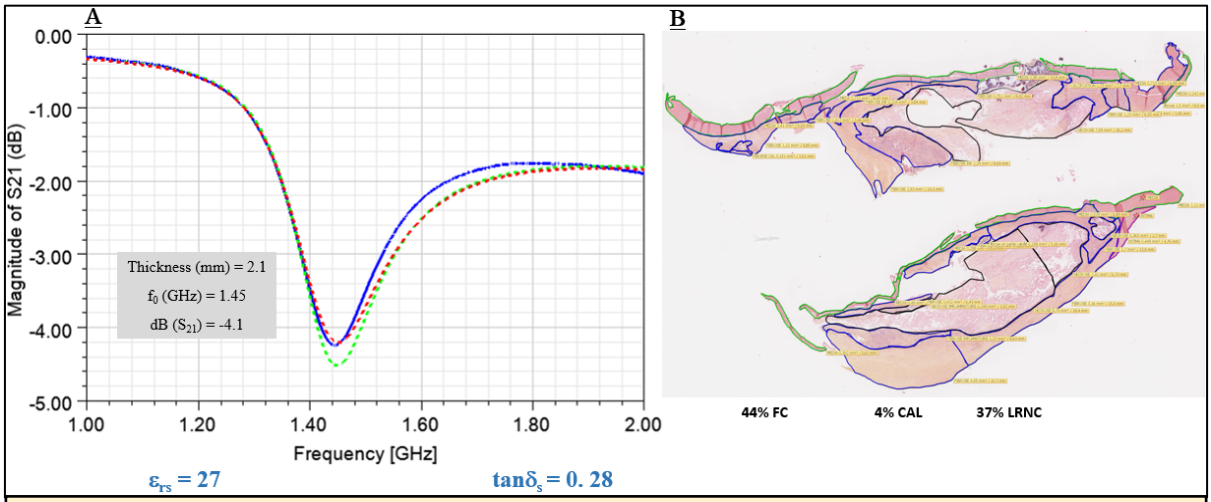

Figure 11. (A) S21 frequency response of a carotid plaque sample of a symptomatic patient. (B) Histological slide analysis of the same patient.

5. Discussion

A variety of imaging modalities and procedures have been developed in recent years to determine the composition of carotid plaques in vivo before performing a CEA in order to assist vascular surgeons in deciding whether or not the operation is justified.

Despite the fact that they are still in the prototype phase, microwave resonators have already produced numerous promising outcomes in the body imaging field [27-29]. Particularly notable for being free from side effects for patients and operators and being easier and cheaper to manufacture [28]. In this cohort research, the performance of a CSRR sensor in distinguishing ex-vivo carotid artery atherosclerotic plaques was tested.

Plaques with elevated levels of calcification displayed significantly lower constant dielectric than plaques with lower levels of calcification and increasing concentrations of LRNC which showed a considerably higher constant dielectric.

The degree of LRNC is typically predictive of ipsilateral stroke risk, which is consistent with results from the patient in figure 10 who had a minor stroke before the procedure and the microwave analysis indicated a constant dielectric value similar to that of blood

This study does have certain restrictions and limitations. First, despite our best efforts to make an accurate comparison between histology and microwave analysis, we cannot say with absolute certainty that the microwave samples precisely represented the histological slides. The microwave samples were significantly smaller and sometimes different from the histological slides.

between the carotid plaques via the constant dielectric from our three analyses is quite accurate.

Second, the performance was assessed using a small sample size consisting of only three patients representing 33 patients; this is due to the time-consuming nature of the histological study of the plaques (in which all deposits are manually graded) and the limited access to patients during the COVID-19 pandemic.

Third, because the samples were kept in physiological serum, the microwave device did not pick up any intraplaque haemorrhage that may have been present and dissolved in the serum. Because of this, the results of the microwave analysis can be affected. In addition, some of the serum might have been trapped inside the plaque and failed to dry over the three minutes, which could alter the results.

In conclusion, even though we found reasonable performance in our microwave device in a preliminary trial with high reproducibility, additional results are required before the microwave sensor can be turned into a diagnostic tool for use in patients.

6. Conclusion and Perspectives

This study illustrated the ability of our device to analyse atheromatous carotid plaques in a standardised way. Calcified plaques displayed very different values from soft lipidic plaques. This ability to differentiate plaques according to their composition is very promising. In the first year of this research project, which is still in progress, 26 asymptomatic and seven symptomatic patients have been examined. The objective is to compare at least 80 patients, 40 from each group. A statistical correlation will be proposed between the histological parameters, the plaques' constant dielectric, and the other radiological modalities based on the results achieved. Multivariate analysis, Bland Altman and Wilcoxson are considered potential statistical methods. In addition, cut-off points to group plaques according to their dielectric permittivity are to be established.

If the hypothesis is proved, the device will be developed into an in-vivo portable device that medical staff could use in hospital settings. To achieve this, a study of multi-layered samples, including skin, fat and the vessel wall, will be considered. Moreover, a parallel feed circular resonator is being considered for larger plaques.

ACKNOWLEDGMENT

We thank Mr Yves Chatelon for his investment in the production of the Plexiglas structure.

[1] K.I. Paraskevas, F.J. Veith, J.D. Spence, How to identify which patients with asymptomatic carotid stenosis could benefit from endarterectomy or stenting, Stroke Vasc. Neurol. 3 (2018) 92–100. https://doi.org/10.1136/SVN-2017-000129.

[2] G. Lanzino, A.A. Rabinstein, R.D. Brown, Treatment of carotid artery stenosis: Medical therapy, surgery, or stenting?, Mayo Clin. Proc. 84 (2009) 362–368. https://doi.org/10.4065/84.4.362.

[3] "*Accident vasculaire cérébral (AVC) – Santé publique France.*" Accessed on: December. 14, 2020. [Online]. Available: https://www.santepubliquefrance.fr/maladies-et-traumatismes/maladies-cardiovasculaires-et-accident-vasculaire-cerebral/accident-vasculaire-cerebral.

[4] A. Chervu, W.S. Moore, Carotid Endarterectomy Without Arteriography, Ann. Vasc. Surg. 8 (1994) 296–302. https://doi.org/10.1007/BF02018179.

[5] H.J.M. Barnett, D.W. Taylor, R.B. Haynes, D.L. Sackett, S.J. Peerless, G.G. Ferguson, A.J. Fox, R.N. Rankin, V.C. Hachinski, D.O. Wiebers, M. Eliasziw., "Beneficial effect of carotid endarterectomy in symptomatic patients with high-grade carotid stenosis.," *N. Engl. J. Med.*, vol. 325, no. 7, pp. 445–453, Aug. 1991.

[6] "Randomised trial of endarterectomy for recently symptomatic carotid stenosis: final results of the MRC European Carotid Surgery Trial (ECST).," The *Lancet*. Vol. 351, no. 9113, pp. 1379–1387, May 1998.

[7] A. Halliday, A. Mansfield, A. Marro, J. Peto, C. Peto, R. Potter, J. Thomas, D. & MRC., "Prevention of disabling and fatal strokes by successful carotid endarterectomy in patients without recent neurological symptoms: randomised controlled trial.," *Lancet (London, England)*, vol. 363, no. 9420, pp. 1491–1502, May 2004.

[8] T. G. Brott *et al.*, "2011 ASA/ACCF/AHA/AANN/AANS/ACR/ASNR/CNS/SAIP/SCAI/SIR/SNIS/SVM/SVS guideline on the management of patients with extracranial carotid and vertebral artery disease: executive summary. A report of the American College of Cardiology Foundation/American Heart Association Task Force on Practice Guidelines, and the American Stroke Association, American Association of Neuroscience Nurses, American Association of Neurological Surgeons, American College of Radiology, American Society of Neuroradiology, Congress of Neurological Surgeons, Society of Atherosclerosis Imaging and Prevention, Society for Cardiovascular Angiography and Interventions, Society of Interventional Radiology, Society of NeuroInterventional Surgery, Society for Vascular Medicine, and Society for Vascular Surgery.," *Circulation*, vol. 124, no. 4, pp. 489–532, Jul. 2011.

Cardoso, and S. Weinbaum, "Revised microcalcification hypothesis for fibrous cap rupture in human coronary arteries.," *Proc. Natl. Acad. Sci. U. S. A.*, vol. 110, no. 26, pp. 10741–10746,Jun. 2013.

[10] J.-M. Davaine *et al.*, "Osteoprotegerin, Pericytes and Bone-Like Vascular Calcification Are Associated with Carotid Plaque Stability," *PLoS One*, vol. 9, no. 9, p. e107642, Sep. 2014, doi: 10.1371/journal.pone.0107642.

[11] T. Funaki, K. Iihara, S. Miyamoto, K. Nagatsuka, T. Hishikawa and H. Ishibashi-Ueda, "Histologic characterisation of mobile and nonmobile carotid plaques detected with ultrasound imaging", *Journal of Vascular Surgery*, vol. 53, no. 4, pp. 977-983, 2011. Available: 10.1016/j.jvs.2010.10.105.

[12] H. Stary, "Natural History and Histological Classification of Atherosclerotic Lesions", *Arteriosclerosis, Thrombosis, and Vascular Biology*, vol. 20, no. 5, pp. 1177-1178, 2000. Available: 10.1161/01.atv.20.5.1177.

[13] H. Stary *et al.*, "A Definition of Advanced Types of Atherosclerotic Lesions and a Histological Classification of Atherosclerosis", *Arteriosclerosis, Thrombosis, and Vascular Biology*, vol. 15, no. 9, pp. 1512-1531, 1995. Available: 10.1161/01.atv.15.9.1512.

[14] L. Saba et al., "Association Between Carotid Artery Plaque Volume, Composition, and Ulceration: A Retrospective Assessment With MDCT", *American Journal of Roentgenology*, vol. 199, no. 1, pp. 151-156, 2012. Available: 10.2214/ajr.11.6955.

[15] M. Reiter *et al.*, "Plaque Imaging of the Internal Carotid Artery—Correlation of B-Flow Imaging with Histopathology," *Am. J. Neuroradiol.*, vol. 28, no. 1, pp. 122 LP – 126, Jan. 2007.

[16] E.L. Chuma, Y. Iano, G. Fontgalland, L.L.B. Roger, H. Loschi, PCB-integrated non-destructive microwave sensor for liquid dielectric spectroscopy based on planar metamaterial resonator, Sensors Actuators, A Phys. 312 (2020). https://doi.org/10.1016/j.sna.2020.112112.

[17] M. Saadat-Safa, V. Nayyeri, M. Khanjarian, M. Soleimani, O.M. Ramahi, A CSRR-Based Sensor for Full Characterisation of Magneto-Dielectric Materials, IEEE Trans. Microw. Theory Tech. 67 (2019) 806–814. https://doi.org/10.1109/TMTT.2018.2882826.

[18] S.K. Singh, N.K. Tiwari, A.K. Yadav, M.J. Akhtar, K.K. Kar, Design of ZnO/N-Doped Graphene Nanohybrid Incorporated RF Complementary Split Ring Resonator Sensor for Ammonia Gas Detection, IEEE Sens. J. 19 (2019) 7968–7975. https://doi.org/10.1109/JSEN.2019.2918304.

[19] A. Javed, A. Arif, M. Zubair, M.Q. Mehmood, K. Riaz, A Low-Cost Multiple Complementary Split-Ring Resonator-Based Microwave

Sens. J. 20 (2020) 11326–11334. https://doi.org/10.1109/JSEN.2020.2998004.

[20] E.L. Chuma, Y. Iano, G. Fontgalland, L.L. Bravo Roger, Microwave sensor for liquid dielectric characterisation based on metamaterial complementary split ring resonator, IEEE Sens. J. 18 (2018) 9978–9983. https://doi.org/10.1109/JSEN.2018.2872859.

[21] J.D. Baena, J. Bonache, F. Martín, R.M. Sillero, F. Falcone, T. Lopetegi, M.A.G. Laso, J. García-García, I. Gil, M.F. Portillo, M. Sorolla, Equivalent-circuit models for split-ring resonators and complementary split-ring resonators coupled to planar transmission lines, IEEE Trans. Microw. Theory Tech. 53 (2005) 1451–1460. https://doi.org/10.1109/TMTT.2005.845211.F.

[22] S. Hardinata, F. Deshours, G. Alquié, H. Kokabi and F. Koskas, "Complementary Split-Ring Resonators for Non-Invasive Characterisation of Biological Tissues," *2018 18th International Symposium on Antenna Technology and Applied Electromagnetics (ANTEM),* 2018, pp. 1-2, doi: 10.1109/ANTEM.2018.8572842.

[23] F. Deshours, G. Alquié, T. Goudjil, H. Kokabi, J-M. Davaine and F. Koskas, “Modélisation de résonateurs en anneaux fendus pour la mesure de permittivités complexes”, XXIèmes Journées Nationales Microondes, Caen, France, 14-17 mai 2019.

[24] S. Hardinata, F. Deshours, G. Alquié, H. Kokabi, F. Koskas, Biosensor miniaturisation for non-invasive measurements of materials and biological tissues, Proc. - 2017 Int. Semin. Sensor, Instrumentation, Meas. Metrol. Innov. Adv. Compet. Nation, ISSIMM 2017. 2017-January (2017) 137–140. https://doi.org/10.1109/ISSIMM.2017.8124278.

[25] Deshours, G. Alquié, J-M. Davaine, L. Aboueb, A. Aissaoui, H. Kokabi. F. Koskas. T. Goudjil, O. Meyer, “Caractérisation microondes de plaques d'athérome calcifiées“. *Journées d'Etude sur la TéléSanté, Sorbonne Universités*, May 2019, Paris, France.

[26] F. Deshours, G. Alquié, H. Kokabi, K. Rachedi, M. Tlili, S. Hardinata, F. Koskas, Improved microwave biosensor for non-invasive dielectric characterisation of biological tissues, Microelectronics J. 88 (2019) 137–144. https://doi.org/10.1016/j.mejo.2018.01.027.

[27] N. Ištuk, E. Porter, D. O'loughlin, B. McDermott, A. Santorelli, S. Abedi, N. Joachimowicz, H. Roussel, M. O'halloran, Dielectric properties of ovine heart at microwave frequencies, Diagnostics. 11 (2021) 1–15. https://doi.org/10.3390/diagnostics11030531.

[28] A. La Gioia, E. Porter, I. Merunka, A. Shahzad, S. Salahuddin, M. Jones, M. O'Halloran, Open-Ended Coaxial Probe Technique for Dielectric Measurement of Biological Tissues: Challenges and Common Practices, Diagnostics. 8 (2018) 40. https://doi.org/10.3390/diagnostics8020040.

microwave imaging for brain stroke followup, Int. J. Antennas Propag. 2014 (2014). https://doi.org/10.1155/2014/312528.

This is an **editable** PDF form. It should **be saved to your computer, then completed** using Adobe reader or equivalent. Please **do NOT substitute** any other document (text file, scanned image, etc.).

Article title : Identification of Carotid Plaques Composition through a Compact CSRR-Based Microwave Sensor

Human and animal rights

☐ The authors declare that the work described has been carried out in accordance with the Declaration of Helsinki of the World Medical Association revised in 2013 for experiments involving humans as well as in accordance with the EU Directive 2010/63/EU for animal experiments.

☑ The authors declare that the work described has not involved experimentation on humans or animals.

Informed consent and patient details

☑ The authors declare that this report does not contain any personal information that could lead to the identification of the patient(s) and/or volunteers.

☐ The authors declare that they obtained a written informed consent from the patients and/or volunteers included in the article and that this report does not contain any personal information that could lead to their identification.

☐ The authors declare that the work described does not involve patients or volunteers.

Disclosure of interest

☑ The authors declare that they have no known competing financial or personal relationships that could be viewed as influencing the work reported in this paper.

☐ The authors declare the following financial or personal relationships that could be viewed as influencing the work reported in this paper:

Funding

☑ This work did not receive any grant from funding agencies in the public, commercial, or not-for-profit sectors.

☐ This work has been supported by:

Author contributions

.

☑ All authors attest that they meet the current International Committee of Medical Journal Editors (ICMJE) criteria for Authorship. Individual author contributions are as follows:

Rania Shahbaz: Carried out the experiment, wrote the manuscript.
Frédérique Deshours: Conducted the simulations.
Georges Alquié: Developed the theory and performed the computations.
Hamid Kokabi : Supervised the electronics part of the project
Isabelle Brocheriou: Verified the histological methods
Gilles Le Naour: Performed the histological analysis
Fabien Koskas : Supervised the medical part of the project
Chaouki Hannachi : Reviewed the manuscript
Jean-Michel Davaine : Designed and directed the project and contributed to the interpretation of the results.

Highlights

- Carotid plaques are identified via the dielectric constant using a microwave sensor.
- The sensor differentiated calcified carotid plaques from plaques at risk.
- A pre-op modality that can identify the composition of the carotid plaque in vivo.
- Correlation of the histological analysis with the dielectric parameters.

Graphical abstract

Identification of Carotid Plaques Composition through a Compact CSRR-Based Microwave Sensor

R. Shahbaz[a,*], F. Deshours[a], G. Alquie[a], H. Kokabi[a], F. Koskas[b], I. Brocheriou[c], G. Le Naour[c], C. Hannachi[a], J.-M. Davaine[b]

[a] *Sorbonne Université, CNRS, Laboratoire Génie Électrique et Électronique de Paris, Paris, France*
[b] *Sorbonne Université, Service de chirurgie vasculaire, Pitié Salpêtrière, Paris, France*
[c] *Sorbonne Université, Service d'Anatomie et cytologie pathologiques, Pitié Salpêtrière, Paris, France*